Scientific Research Publishing

Advances in Materials Physics and Chemistry, 2024, 14, 196-212
https://www.scirp.org/journal/ampc
ISSN Online: 2162-5328
ISSN Print: 2162-531X

Allophane as a Nanotechnological Additive in Masonry Materials to Increase Resistance and Waterproofing

Edward H. Jiménez[1*], Joao Rivera[1], Juan H. Villalba[1], Paola E. Vera[1], Marlon Cuenca[2], Belén Granja[2], Javier Fuentes[2], Sandra Gavilanes[1], Daniel Hidalgo[1], Fernando Garcia[1], Jose Bermudez[1], Washington Ruiz[1], Alexis Martial Debut[3]

[1]Facultad de Ingeniería Química, Universidad Central del Ecuador, Quito, Ecuador
[2]Facultad de Arquitectura y Urbanismo, Universidad Central del Ecuador, Quito, Ecuador
[3]Nanomaterials Characterization Laboratory, Universidad de las Fuerzas Armadas ESPE, Sangolquí, Ecuador
Email: *ehjimenez@uce.edu.ec

How to cite this paper: Jiménez, E.H., Rivera, J., Villalba, J.H., Vera, P.E., Cuenca, M., Granja, B., Fuentes, J., Gavilanes, S., Hidalgo, D., Garcia, F., Bermudez, J., Ruiz, W. and Debut, A.M. (2024) Allophane as a Nanotechnological Additive in Masonry Materials to Increase Resistance and Waterproofing. *Advances in Materials Physics and Chemistry*, **14**, 196-212.
https://doi.org/10.4236/ampc.2024.148015

Received: July 6, 2024
Accepted: August 27, 2024
Published: August 30, 2024

Abstract

The constant need for high-strength materials in the construction industry promotes the research of additives that improve the properties of masonry materials. The use of allophane as an additive in concrete and mortar mixtures was implemented to improve their strength and waterproofing, respectively, using compression and water absorption tests according to their corresponding standards (ASTM C1231, ASTM D2938, and ASTM C1585). The samples were evaluated at different concentrations and curing ages. In addition, different sand/cement ratios were considered for the mortar. The results revealed that there was a 9.4% increase in compressive strength in concrete and a 23.7% reduction in water absorption in mortar for the 5:1 ratio. These changes would be the result of the interaction of the nanoporous additive in the atomic crystal structure of the material demonstrating the nanotechnological nature of allophane.

Keywords

Allophane, Nano Additive, Strength, Impermeability, Concrete, Mortar

1. Introduction

In the construction industry, different types of problems are evidenced as surface defects in civil works, as a consequence of the changes that concrete undergoes, due to physical, mechanical, chemical, or biological effects, which affect durability and structural properties [1].

To improve the quality of masonry materials and reduce construction costs, additives are implemented in the mixing process, modifying their properties

such as the reduction in water content [2], allowing very low water/cement ratios to be obtained, as well as promoting the setting and hardening of concrete, reducing formwork stripping time, among others.

Research on different types of admixtures has focused on mineral compounds of natural origin with silica and aluminum content. Clinoptilolite, a type of zeolite, has been studied for the modification of mortar behavior against moisture, showing promising results [3]. On the other hand, micro and nano silica have been studied in compressive strength and capillarity in cementitious mixtures [4] [5].

Allophane is an amorphous mineraloid composed of aluminum silicate with no defined crystalline structure. Its idealized formula is $Al_2O_3(SiO_2)_{1.3\text{-}2}\cdot(2.5\text{-}3)H_2O$, which is characterized by its Si/Al ratio that in the Ecuadorian case is between 1.45 and 1.85. It has a large surface area, high porosity and variable charge. Due to its high specific surface area, allophane can have diverse applications such as phosphate and water retention, water remediation, adsorption, and as an additive for fertilizers [6].

The present research seeks to implement allophane as an additive for masonry materials and evaluate its properties in terms of compressive strength and moisture absorption, depending on the concentration of allophane used, since it possesses similar characteristics to Pozzolans [7] being mineral additives capable of affecting the hydration kinetics of cement [8], and the reduction of water content leading to a decrease in total porosity [9].

2. Methodology

2.1. Cementitious Pastes

2.1.1. Maintaining the Integrity of the Specifications

It is a homogeneous mixture of fine inorganic aggregates, cement, and water, used in construction with wide applications in masonry according to its dosage [10]. According to their cement: sand ratio, they are classified according to their use as shown in **Table 1**.

Table 1. Cement: sand ratios and uses.

Mortar	Uses
1:1	Very rich mortar for waterproofing. Fillings.
1:2	For waterproofing and subway tank diphragms and Backfill.
1:3	Minor waterproofing. Floors.
1:4	Wall brick and tile adhesive. Fine masonry.
1:5	Exterior masonry. Bonding for bricks and tiles, brickwork and masonry in general. Not very thin masonry.
1:6 and 1:7	Interior masonry. Glue for bricks and tiles, brickwork and masonry in general. Not very thin masonry.
1:8 and 1:9	Sticks for construction to be demolished soon. Stabilization of slopes in foundations.

Source: [11].

Design

Dosages were designed by ASTM C 270-14 (American Society for Testing and Materials) [12], which specifies that laboratory tests should be carried out in mass ratios. For the experimentation, the ratios 1:3, 1:4 and 1:5 were considered, using as fine aggregate, blue powder and Portland cement type GU by NTE INEN 2380 (Instituto Ecuatoriano de Normalización) [13].

The amount of water required for the dosage was defined experimentally until the workability of the mixture was achieved, by standard NTE INEN 2518 [14]. Table 2 details the dosage for the mortar for the three ratios and additive concentrations from 0 to 2%. To confirm that the effect of the additive in the mixture is different from that of the cement, a sample with an additional 1.5% binder was added, as shown in Table 2.

Table 2. Dosage for 50 × 50 mm mortar samples.

Ratio	Additive (%)	Cement (g)	Blue powder (g)	Water (ml)
1:3	0	140	420	93
	0.5			98
	1			97
	1.5			100
	2			101
	1.5 C[a]			95
1:4	0	115	460	95
	0.5			95
	1			96
	1.5			95
	2			96
	1.5 C[a]			98
1:5	0	95	475	94
	0.5			94
	1			93
	1.5			96
	2			94
	1.5 C[a]			94

[a]Addition of cement instead of additive.

2.1.2. Concrete

It is a homogeneous mixture of binder, water, and fine and coarse aggregates. It is currently the most widely used material in the construction industry because of its durability, strength, impermeability, ease of production, and economy [11].

Design

For the design of 1 m^3 of concrete, the characterization of fine and coarse aggregates was carried out based on the ASTM C33 [15], C128 [16], C136 [17], C 127 [18], C 566 [19], C 29 [20], C 131 [21], C 40 [22], as shown in **Table 3** and **Table 4**.

Table 3. Characterization of aggregates per cubic meter.

Materials	Coarse aggregate	Fine aggregate
(%) Moisture	4.41	3.00
(%) Absorption	3.47	3.28
SSS State	631.20	771.47
Dry State	610.02	746.94
Natural state	636.91	769.32
Cement	568.73	
Net water	255.93	
Mixing water	252.38	

Table 4. Dosage for a test specimen.

Cement, kg	Water, kg	Blue powder, kg	Coarse aggregate, kg	Additive, %
1.786	0.793	2.417	2.00	0
				0.13
				0.17
				1.00

2.2. Nanotechnological Additive

2.2.1. BET Area and Particle Size

As part of the characterization of the allophane, surface area analyses were carried out using the BET technique using a Chemisorption of MICROMETRICS analyzer, following ASTM E11 [23] and using three particle size fractions of 45, 106, and 425 μm, obtained by sieving. Before exposure to the inert gas, a degassing process was applied to the samples to eliminate any surface contaminant.

2.2.2. SEM and TEM Analysis

To complement the structural and morphological characterization of the nanomaterial two electron microscopy techniques were used: the scanning electron microscope, with a Tescan-MIRA 3 model, and the transmission electron microscope, with an FEI-Tecnai Spirit Twin (120 kV) model. These analyses were carried out on samples with the same physical separations used in the BET analysis. Subsequently, a frequency distribution study was performed based on sub-particle measurements observed in the TEM analysis and measured with the Fiji software, in order to identify their size.

2.3. Obtaining the Diffractograms of Concrete, Allophane Nanoparticles and Size Determination Using the Scherrer Equation

Three samples were tested pure allophane and concrete with and without additives, for which it was necessary to reduce the particle size of each of the samples for subsequent sieving to ensure uniformity.

The X-ray diffractometer (XRD) Panalytical-Empyrean of the Laboratory of Characterization of Nanomaterials of the University of the Armed Forces (ESPE) was used.

The result of the interaction between the emitted X-rays and the sample structure gives us a diffractogram that, once interpreted, identifies the structure of crystalline materials and the short-range order of non-crystalline materials. [24].

For the calculation of the average size of the nanocrystals, first, a peak fitting of the diffractogram was performed using the voigt function of the OriginLab 2024 software and the average crystallite size was determined using the Scherrer equation.

The Scherrer equation is used in crystallography to estimate the average size of crystals in a material [25] from the width of peaks in an X-ray diffraction pattern. The equation is expressed as follows:

$$L = \frac{K\lambda}{\beta \cdot \cos\theta} \tag{1}$$

Follow:

L = Crystallite size (nm);

K = Scherrer constant (depends on crystalline form);

λ = X-ray wavelength (Å);

β = FWHM (Full width at half maximum);

θ = Angular position of peaks (Bragg), half of 2-theta 2θ.

2.4. Compressive Strength

2.4.1. Compressive Strength in Concrete

For the tests, 10 × 20 cm cylinders were made with the experimental design proposed in point 2.1.2.1, following the ASTM C39 [26] and ASTM C1231 [27] protocol at seven days of curing, using sieved allophane with physical separation of 106 μm. The experimentation was performed in triplicate. It is important to emphasize that the study was carried out only at early ages because previous research showed that the maximum peak of resistance concerning the standard was reached in this period [28].

2.4.2. Compressive Strength in Mortar

Cubes of 50 mm edge were tested according to ASTM D2938-950 [29], following the experimental design presented in section 2.1.1.1, at the same age as the concrete tests, with allophane from the 425 μm physical separation sieve. They were tested in duplicate.

2.5. Maximum Initial Absorption and Absorbance in Mortars

The 50 mm cubes were tested according to ASTM C1585 [30], using allophane from the 425 μm sieve of physical separation; at 7 and 28 days of curing. The tests were performed in duplicate.

3. Results and Discussion

3.1. BET Area and Particle Size

The results of the BET analysis revealed the presence of nanopores in the material, which was reflected in the high gas adsorption capacity at various pressures during the analysis, indicating an active surface and a significant porous structure.

These findings suggest that nanoporous admixture has the potential to improve the properties of construction materials, such as concrete and mortar, by providing a larger surface area for physicochemical interactions and a higher water-holding capacity [31]. The results obtained for the three types of admixture analyzed are shown in Table 5.

Table 5. Physical-chemical characterization of allophane

Chemisorption (cm^3/g)	85,828	88,604	87,885
BET (m^2/g)	46,614	81,537	45,006
			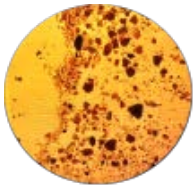
Particle (μm)	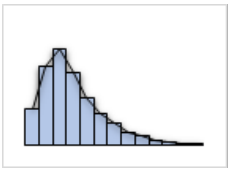	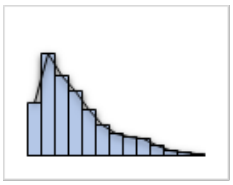	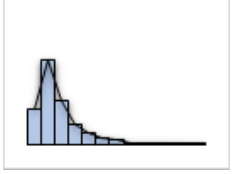
	μ = 18.111 N = 7000	μ = 39.431 N = 5400	μ = 80.71 N = 3400
Physical separaction, μm	45	106	425

The incorporation of nanopores into the masonry mix can offer a potential improvement by increasing its specific surface area [32], which, in turn, increases its capacity to adsorb moisture from the surrounding air, causing the material to maintain a more stable relative humidity inside the structure.

On the other hand, nanopores can modify the capillary structure of the material, which would affect how water moves within it. In addition, they can make it more difficult for water to penetrate deeply [33]. Finally, they can act as water reservoirs during the preparation of the material mix, allowing the allophane to

act as an internal curing agent, which would contribute to improving its durability and strength [34].

3.2. SEM and TEM Analysis

The images obtained by SEM analysis reveal the surface morphology of the nanomaterial. Observing for the three types of samples an amorphous configuration without a defined crystalline structure, typical of aluminosilicates. The particles show an irregular and rough shape. There is no observable atomic ordering, as shown in columns (a), (b), and (c) of **Figure 1**.

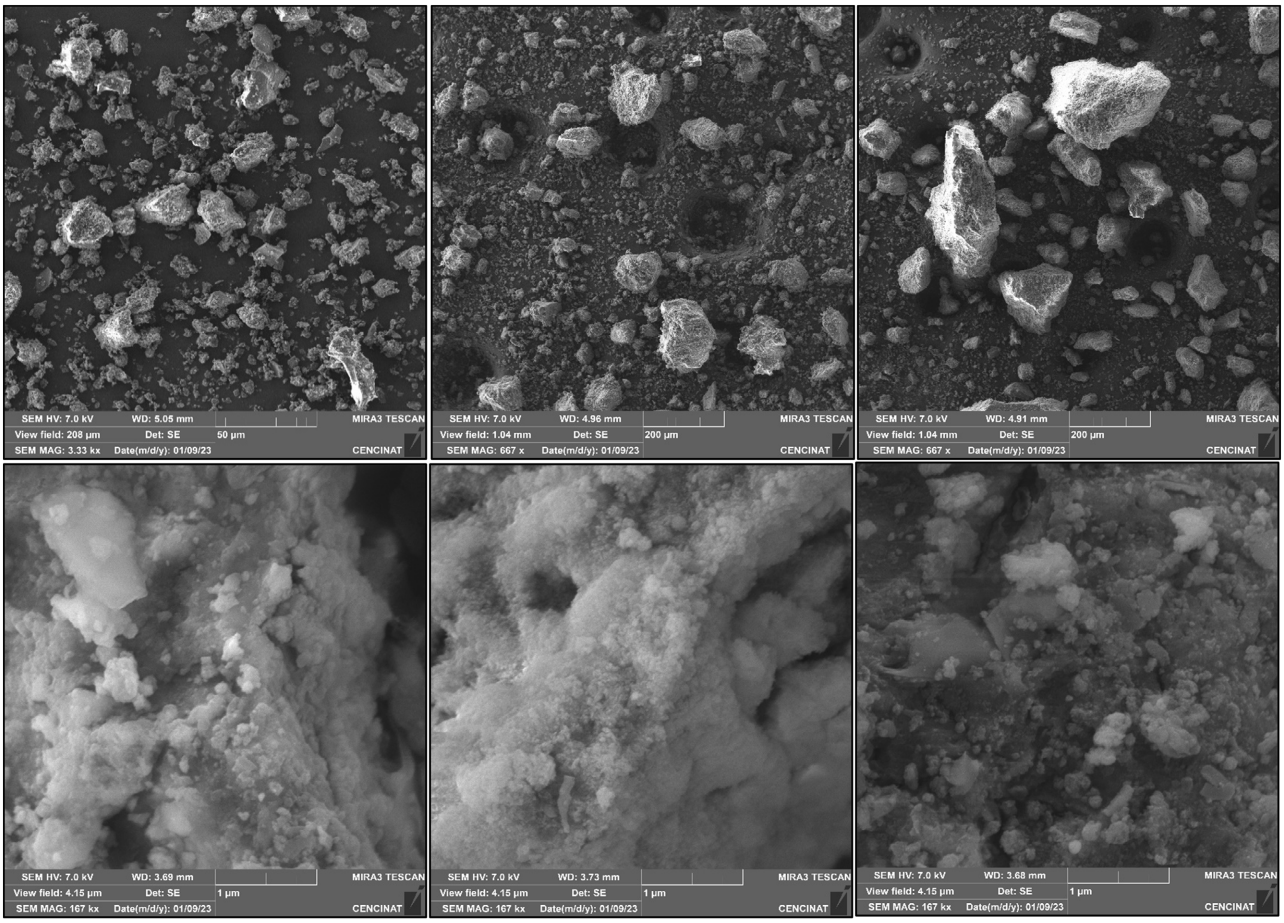

Figure 1. Images of SEM analysis of allophane particles. Each physical separation is represented by column (a), (b) and (c), corresponding to 45 µm, 106 µm and 425 µm, respectively.

On the other hand, the images obtained in the TEM analysis (**Figure 2**) show details of the additive at a nanometer scale, evidencing the presence of sub-particles forming conglomerates, found between 3.2 and 3.8 nm and showing a variable density, suggesting a heterogeneous composition. No defined crystalline structures are identified, confirming the amorphous nature of the material. Finally, no porosities were visualized in the samples which is far from the results obtained in the BET analysis, which showed a high surface area.

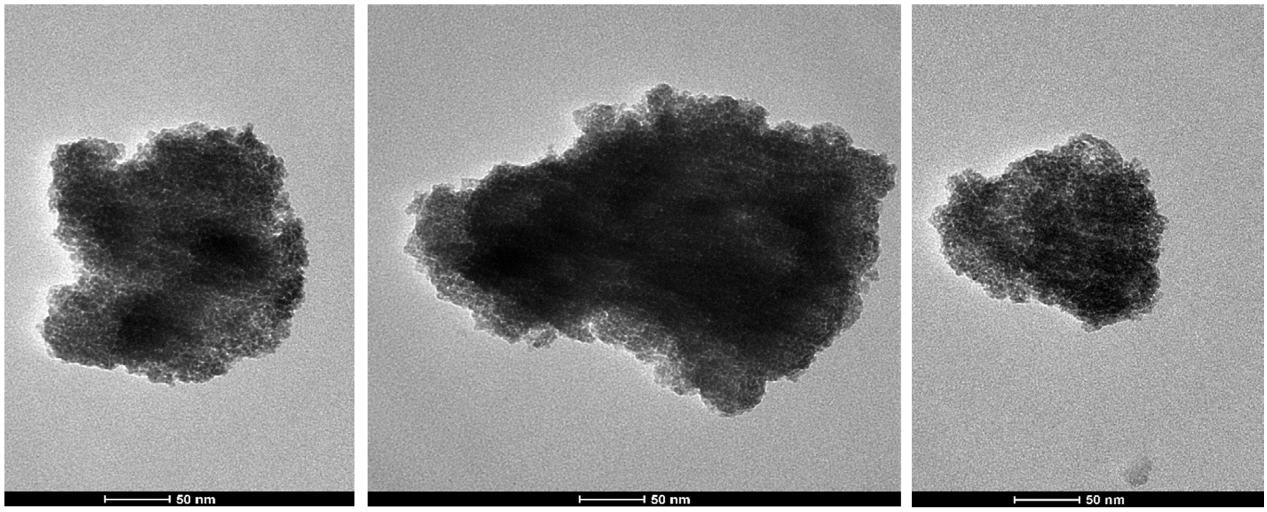

Figure 2. Images of TEM analysis of allophane particles. Each physical separation is represented by column (a), (b) and (c), corresponding to 45 μm, 106 μm and 425 μm, respectively.

The non-crystalline nature of the additive could offer multiple advantages in the structural properties of building materials [35]. This structural complexity may result in greater flexibility in interaction with the components of the mixture, which would facilitate their uniform dispersion in the matrix of the building material. These allophane particles are prone to form highly porous micro aggregates [36].

On the other hand, the characterization of the material allowed determining the presence of nanoparticles that form allophane conglomerates; their external diameter is between 3.2 and 3.8 nm from Fiji analysis, which coincides with previous characterization analyses that indicate that these nanoparticles have diameters between 3 and 5 nm [37], as shown in **Figure 3**.

In a nanoparticle size distribution with positive skew, most nanoparticles are small, but there are some that are much larger. This distribution has a longer tail to the right, indicating that although the average size is low, there are significantly larger nanoparticles that influence the skew.

It should be noted that the porosities described in the BET analysis are not perceptible with the microscopy techniques used, suggesting the presence of a nanoporous structure, which should be found in an estimated pore diameter of less than 1 nm [38]. This characteristic increases the adsorption capacity and the microstructure of the material, which would benefit both its physicochemical and mechanical properties.

3.3. Crystallography-Size Determination Using Scherrer's Equation

Characterization by X-ray diffraction identifies the crystalline phase or phases present in the analyzed sample. The result of the refraction of the beam by a material that has an atomic arrangement in its crystal lattice [25]. The beams

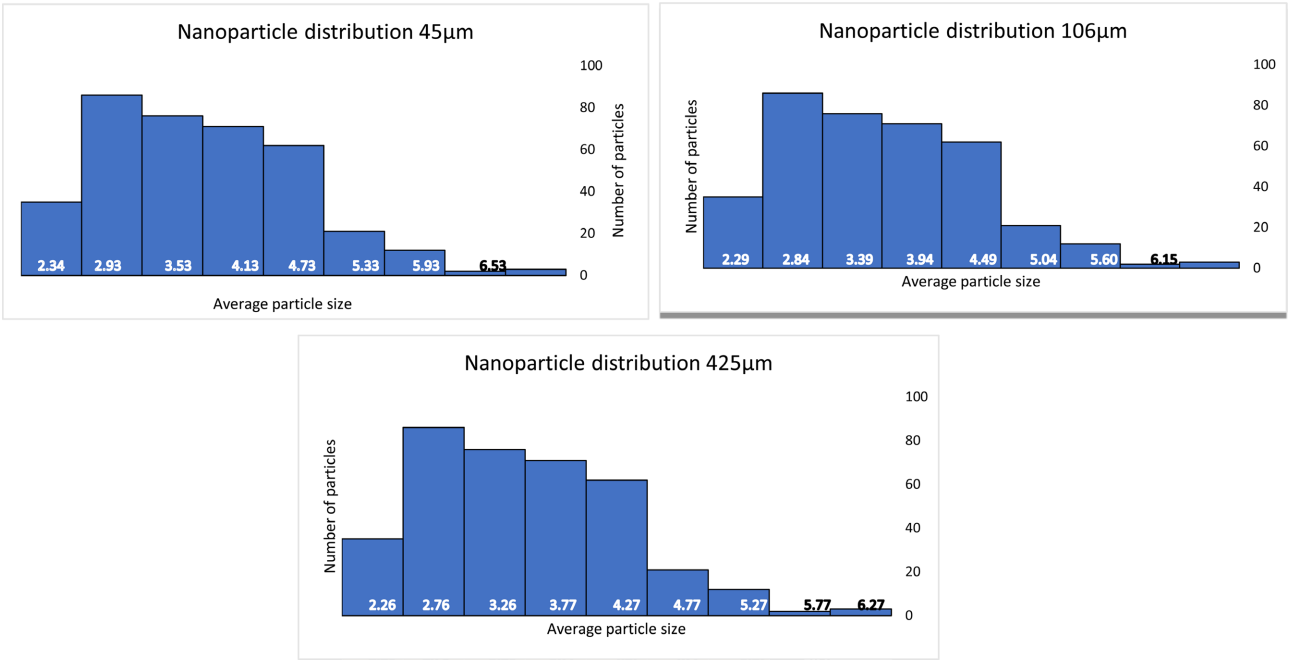

Figure 3. Frequency distribution of the diameter of clustered allophane nanoparticles.

diffract and form certain patterns called fingerprints [39].

Applying Scherrer's equation to characterize the crystallography of concrete, the value of the constant K = 0.89 for spherical and porous allophane particles was proposed [37], yielded a crystallite size of 18.79 nm (**Table 6**) and for the concrete with admixture a value of 19.79 nm (**Table 7**), evidencing that there is an interaction by the admixture that is influencing the microstructure of the concrete.

Table 6. Average crystal size for standard concrete.

K	λ (Å)	#	Peak position 2θ (˚)	Average FWHM B (˚)	L (nm)	Average of 3 peaks:	16.23
0.89	1.54	1	20.81	0.391	20.38	Total average:	19.79
		2	21.93	0.415	19.25		
		3	23.65	0.357	22.45		
		4	24.48	0.365	22.02		
		5	26.57	0.482	16.71		
		6	27.81	0.509	15.89		
		7	29.36	0.504	16.09		
		8	31.49	0.402	20.28		
		9	39.48	0.411	20.27		
		10	48.46	0.390	22.04		
		11	67.84	0.423	22.33		

Table 7. Average crystal size for admixed concrete.

K	λ (Å)	#	Peak position 2θ(˚)	Average FWHM B (˚)	L (nm)	Average of 3 peaks:	15.13
0.89	1.54	1	20.83	0.4210	18.97	Total average:	18.79
		2	21.94	0.435	18.37		
		3	23.66	0.375	21.39		
		4	26.58	0.486	16.59		
		5	27.90	0.604	13.38		
		6	29.36	0.526	15.43		
		7	36.74	0.420	19.70		
		8	39.40	0.411	20.29		
		9	48.45	0.387	22.22		
		10	50.03	0.401	21.61		

The Scherrer Equation does not apply to allophane, since it does not have a defined crystalline structure. This is because it presents a predominant amorphous area between the peaks and along the diffractogram, according to the XRD study of [40] for quantitative analysis of materials.

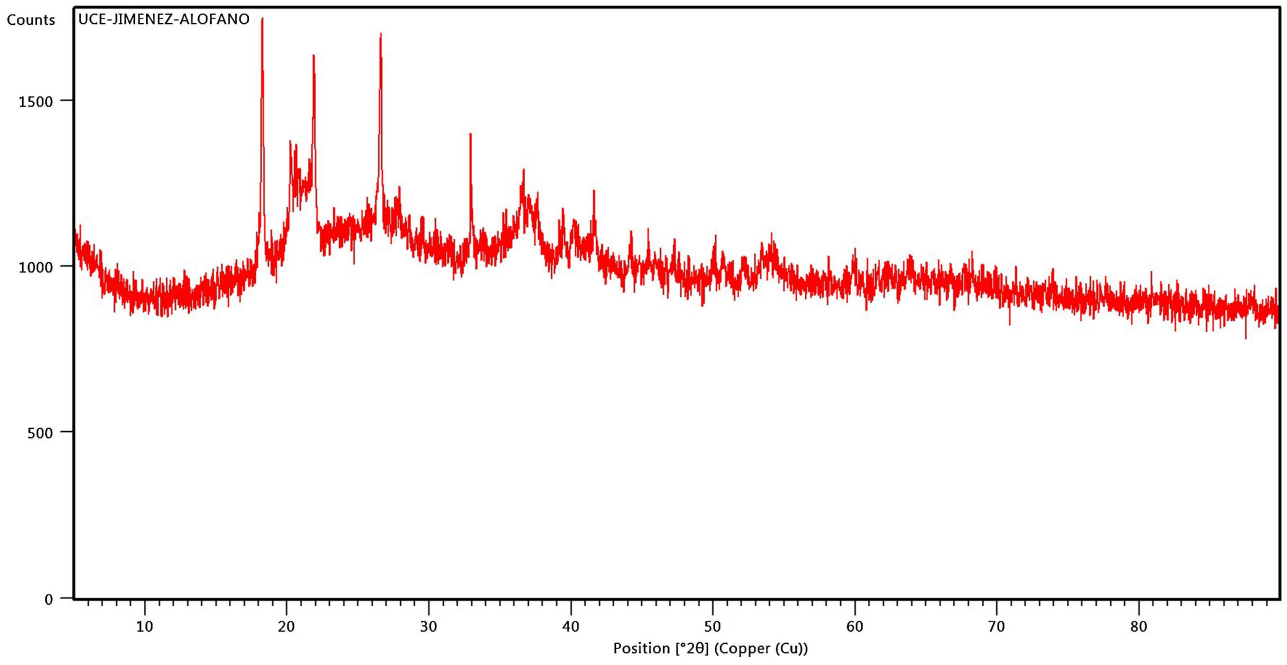

Figure 4. Allophane diffractogram.

The diffractogram (**Figure 4**) shows reflections of amorphous characteristics because no clear diffraction pattern is found. But it presents three broad bands with intensities of strong, medium, and weak; similar to the allophane samples described in the research of [41]. However, there are some differences due to the

impurities in the allophane used in that experiment.

For the diffractograms obtained from the concrete standard sample (Figure 5) and the additized concrete (Figure 6), modifications are observed in some peaks that suggest changes in the crystalline structure.

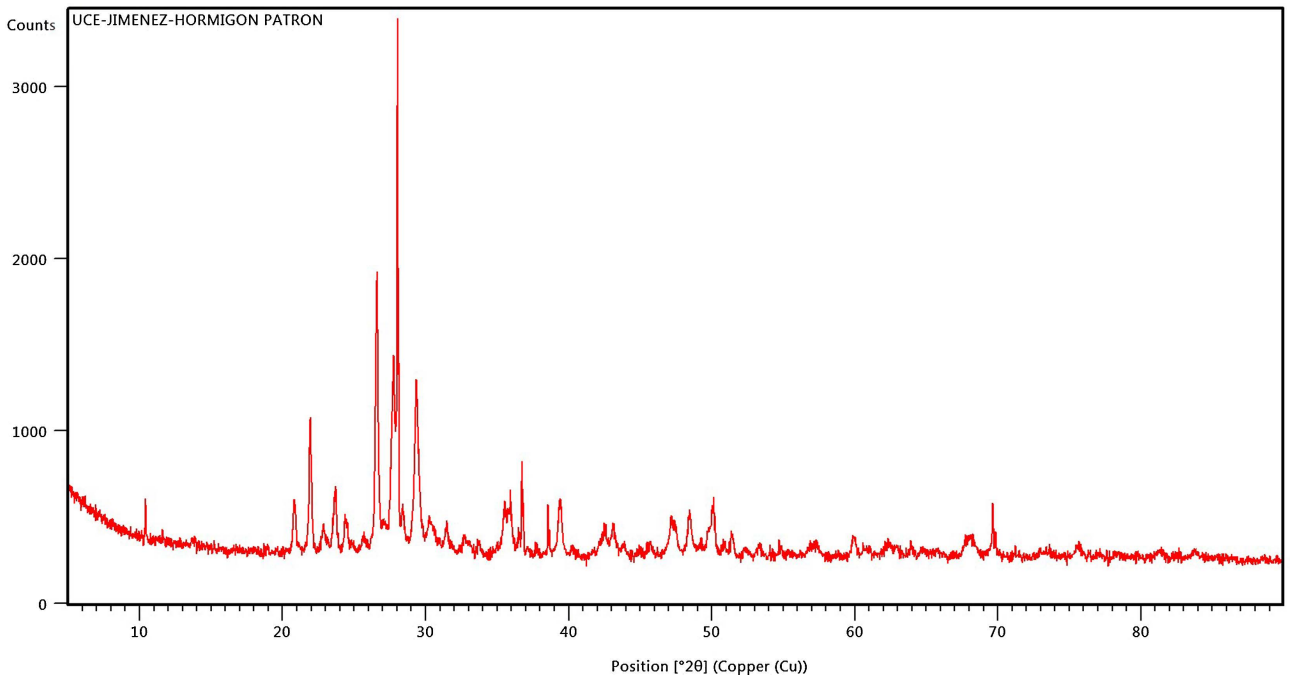

Figure 5. Diffractogram of the standard concrete sample.

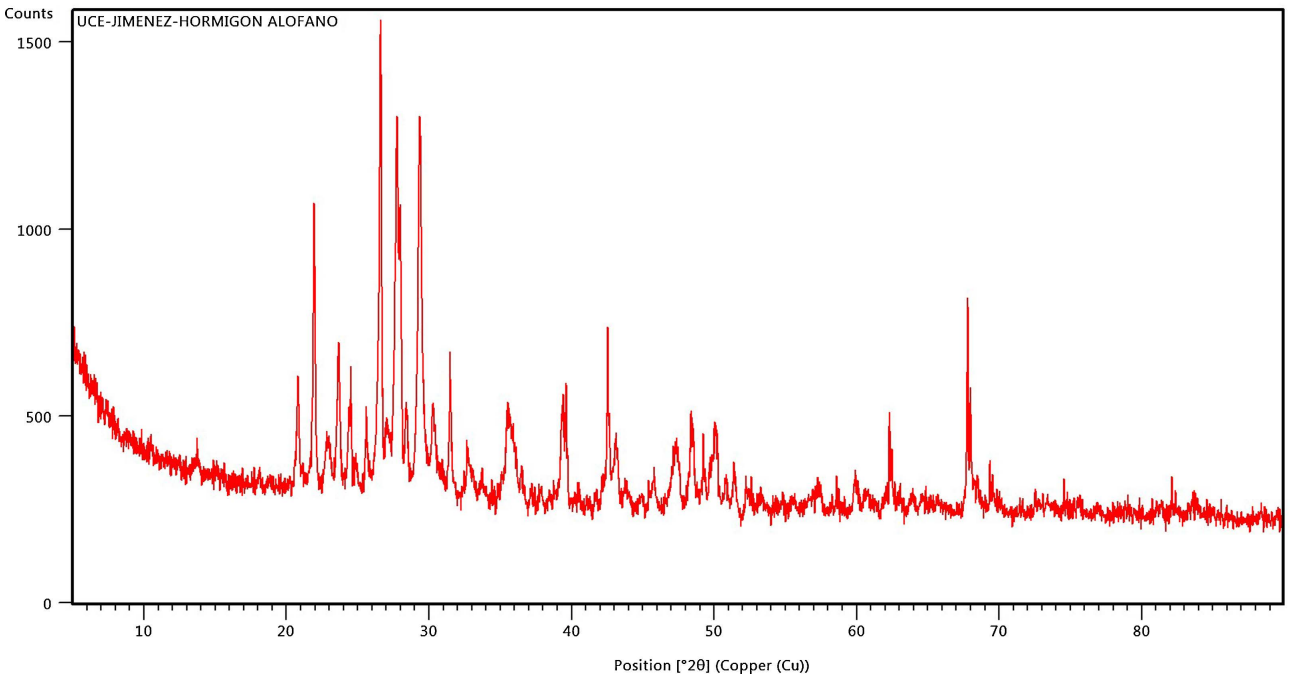

Figure 6. Diffractogram of the concrete sample with allophane.

It may be that the admixture used in the concrete promotes more significant

crystalline growth or less crystalline deformation than the standard concrete.

Due to the specific nature of the admixture, allophane being an andosol, a consequence of weathering processes under acidic conditions in humid climates [37] and supergene processes such as tephra-disturbed soils and leached layers, appears as an aggregate of hollow nanospheres [42], its pores (0.35 - 0.5 nm) and coarse surface area, give it a high adsorption capacity [43], giving it distinctive characteristics of volcanic soils such as water retention, which depends mainly on the texture and the presence or not of non-crystalline aluminosilicates [44].

In this way, allophane participates as an internal curing agent, allowing nano-level interactions with the components that make up the concrete. Rheological properties (viscosity/time/resistances) and hydration properties (nucleation and crystalline growth) are crucial during the setting process because of their effects on the final appearance and the strength and durability of the concrete [45].

Figure 5 and **Figure 6**, show that allophane influences the microstructure of concrete, which in turn affects the size and distribution of crystallites and, therefore, could promote a better dispersion of cementitious materials, resulting in a more homogeneous microstructure with larger crystals in the concrete with admixture.

3.4. Influence of the Admixture Concentration on the Compressive Strength of Concrete

The addition of allophane to concrete results in an increase in compressive strength, as seen in, with the largest increase being 9.4% for the additive concentration of 0.13%, in relation to (**Figure 7**) its standard sample.

The resistance obtained in the standard samples differs from each other because the tests were carried out in different environmental conditions and times

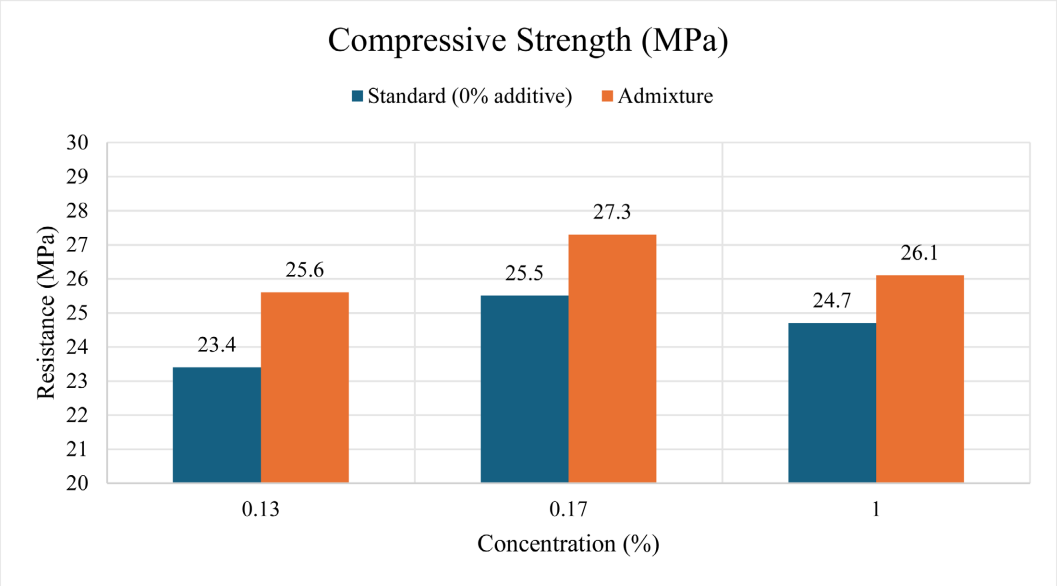

Figure 7. Comparison of compressive strength in concrete.

of the year, which is why the parameter of analysis is the increase in resistance in each test.

Comparing these results with the difference in crystallite size of the sample with additive and the standard, it can be presumed that this effect is due to the nanotechnological influence of allophane in the crystalline structure of the material.

3.5. Influence of Admixture Concentration on Compressive Strength in Mortar

Figure 8 shows that the admixture, at any concentration, decreases the compressive strength, regardless of the cement: sand ratios, the maximum decrease for each ratio being 36.64% for 1:3, 41.15% for 1:4, and 28.78% for 1:5.

However, this compressive strength was evaluated at early ages; therefore, it is not conclusive at older ages. The lowest percentage decreases were found in the 1:5 ratio at low additive concentrations.

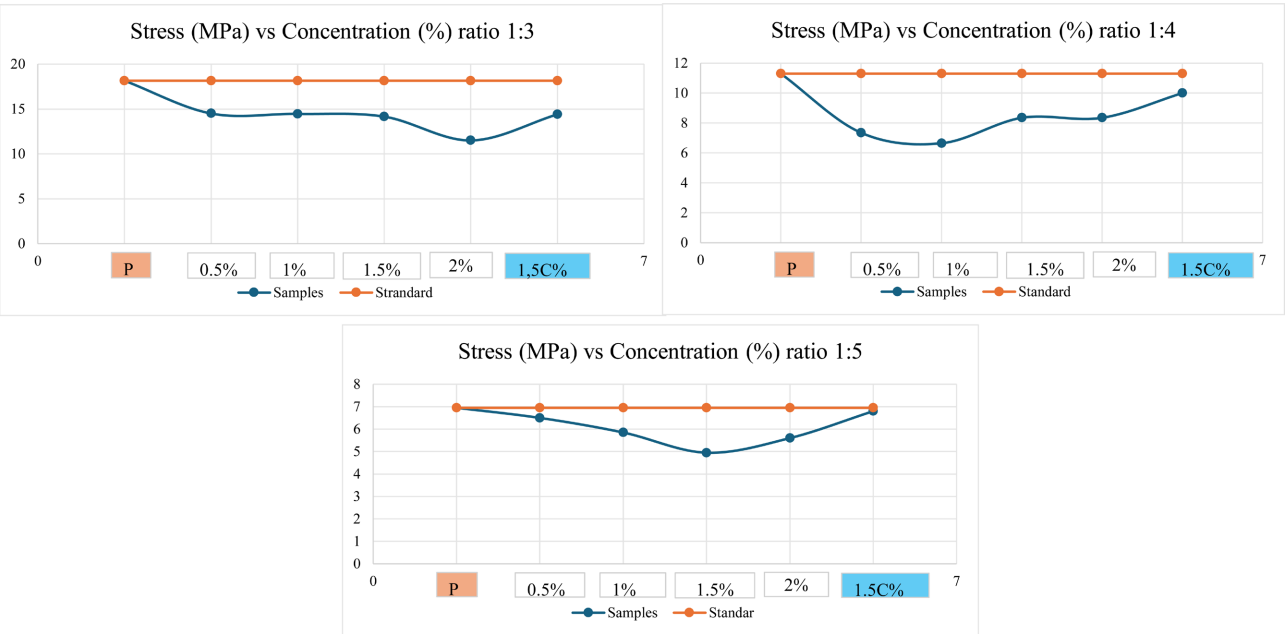

Figure 8. Stress for different admixture concentrations in mortar.

3.6. Influence of Admixture Concentration on Maximum Initial Absorption and Absorption in Mortars

Figure 9 shows that, with one week of curing, the absorption behavior is unpredictable, being so, that the curves in the different ratios do not present a single optimum concentration, where the absorption of water by capillarity is prevented in the samples concerning the standard.

On the contrary, at the age of 28 days of curing, it is observed that in the 1:5 ratio, the concentration of 0.5% has the lowest absorption concerning the standard, thus being the dosage with the best-obtained results.

On the other hand, the implementation of a specimen with the presence of

cement in substitution of the additive (1.5% C), in all cases presents higher absorption than the standard, which shows that the additive provides properties different from those of the binder powder used.

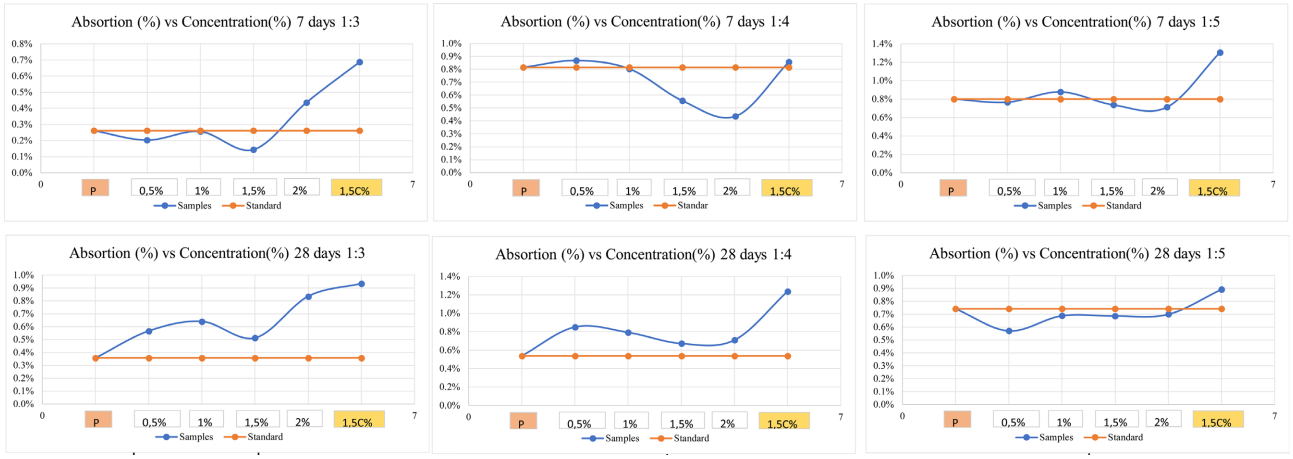

Figure 9. Time-dependent fusion absorption for different ratios at 7 and 28 Days.

4. Conclusions

The implementation of allophane as an additive represents an improvement in the properties of masonry mixtures, causing interactions with the material that generate stable compounds during the mixing process, thus improving the strength and durability of the material.

Allophane influences the microstructure of concrete, which in turn, affects the size and distribution of crystallites. The admixture could promote better dispersion of the cementitious materials, resulting in a more homogeneous microstructure with larger crystallites in the admixture mix. If the admixed concrete has larger crystals, it would indicate better consolidation of the material and a more robust structure. Consequently, the concrete with admixture has better mechanical strength and durability compared to the standard. The highest increase was 9.4% in the sample with 7 days of curing with a concentration of 0.13% of admixture (see **Figure 7**).

The influence of the additive concentration on the crystallite size is reflected in a macroscopic property such as compressive strength, thus evidencing the nanotechnological effect of allophane on the crystalline structure of the material.

The addition of allophane to the mortar can reduce moisture absorption, but the effectiveness of this effect depends on the concentration of the additive, the proportion of cement and sand, and the curing time. Showing better results, the mix with 5:1 w/c ratio, 0.5% admixture at 28 days of curing (see **Figure 9**). These findings support the use of allophane as an admixture in mortars to improve their moisture resistance but suggest the need to adjust the admixture concentration according to the specific application conditions and material proportions.

The results obtained from the properties analyzed suggest that the nanopo-

rous structure of the allophane particle affects the internal activity of the mixture, thus acting as an internal curing agent and facilitating more complete hydration in the mixture; this contributes to a denser and stronger matrix in the final concrete and helps form a more cohesive structure, which reduces porosity and increases the impermeability of the material.

Conflicts of Interest

The authors declare no conflicts of interest regarding the publication of this paper.

References

[1] Wang, R., Zhang, Q. and Li, Y. (2022) Deterioration of Concrete under the Coupling Effects of Freeze–Thaw Cycles and Other Actions: A Review. *Construction and Building Materials*, **319**, Article 126045. https://doi.org/10.1016/j.conbuildmat.2021.126045

[2] Saedi, A., Jamshidi-Zanjani, A. and Darban, A.K. (2021) A Review of Additives Used in the Cemented Paste Tailings: Environmental Aspects and Application. *Journal of Environmental Management*, **289**, Article 112501. https://doi.org/10.1016/j.jenvman.2021.112501

[3] Flores-Lozano, E.S., López-de Juambelz, I.R., Velázquez-Vázquez, D., Moreno-Pérez, E. and Hernández-Ávila, J. (2021) Modificación del comportamiento del mortero con respecto a la humedad por adición de zeolita. *Pädi Boletín Científico de Ciencias Básicas e Ingenierías del ICBI*, **9**, 193-200. https://doi.org/10.29057/icbi.v9iespecial2.8008

[4] Mendoza, J. (2018) Influencia Del Porcentaje, Tipo Y Dosificación De Microsílice En La Resistencia A La Compresión Y Capilaridad En Morteros Elaborados Con Cemento Tipo V.

[5] Tobón, J.I., Restrepo Baena, O.J. and Payá Bernabeu, J.J. (2007) Adición de nanopartículas al cemento Portland. *DYNA*, **152**, 277-291. https://revistas.unal.edu.co/index.php/dyna/article/view/930

[6] Jimenez, E., López, A., Gonzáles, H., Calle, L., Ochoa, P. and Stahl, U. (2024) Físicoquímica de los Alofanos y sus aplicaciones en la refinación de crudo. Universidad Central del Ecuador, 2019. https://isbn.cloud/9789942945822/fisicoquimica-de-los-alofanos-y-sus-aplicaciones-en-la-refinacion-de-crudo/

[7] Ortega, M. (2021) Análisis de propiedades físico—Mecánicas de lechadas de cemento con 'alófano' para la sección superficial de pozos de petróleo.

[8] Kapeluszna, E., Szudek, W., Wolka, P. and Zieliński, A. (2021) Implementation of Alternative Mineral Additives in Low-Emission Sustainable Cement Composites. *Materials*, **14**, Article 6423. https://doi.org/10.3390/ma14216423

[9] Kujawa, W., Olewnik-Kruszkowska, E. and Nowaczyk, J. (2021) Concrete Strengthening by Introducing Polymer-Based Additives into the Cement Matrix—A Mini Review. *Materials*, **14**, Article 6071. https://doi.org/10.3390/ma14206071

[10] Santos, T., Almeida, J., Silvestre, J.D. and Faria, P. (2021) Life Cycle Assessment of Mortars: A Review on Technical Potential and Drawbacks. *Construction and Building Materials*, **288**, Article 123069. https://doi.org/10.1016/j.conbuildmat.2021.123069

[11] Gutiérrez de López, L. (2003) El concreto y otros materiales para la construcción. Universidad Nacional de Colombia.

[12] American Society for Testing and Materials (2024) Standard Specification for Mortar for Unit Masonry.

[13] Instituto Ecuatoriano de Normalización (2011) Cemento Hidraúlico. Requisitos de desempeño para cementos hidraúlicos.

[14] INEN (2010) Morteros para unidades de mampostería. Requisitos.

[15] ASTM (2023) Standard Specification for Concrete Aggregates.

[16] ASTM (2023) Standard Test Method for Density, Relative Density (Specific Gravity), and Absorption of Fine Aggregate.

[17] ASTM (2020) Standard Test Method for Sieve Analysis of Fine and Coarse Aggregates.

[18] ASTM (2024) Standard Test Method for Relative Density (Specific Gravity) and Absortion of Coarse Aggregate.

[19] ASTM (2019) Standard Test Method for Total Evaporable Moisture Content of Aggregate by Drying.

[20] ASTM (2017) Standard Test Method for Bulk Density ('Unit Weight') and Voids in Aggregate.

[21] ASTM (2010) Standard Test Method for Resistance to Degradation of Small-Size Coarse Aggregate by Abrasion and Impact in the Los Angeles Machine.

[22] ASTM (2011) Standard Test Method for Organic Impurities in Fine Aggregates for Concrete.

[23] ASTM (2022) Designation: E11-22 Standard Specification for Woven Wire Test Sieve Cloth and Test Sieves 1.

[24] Khan, H., Yerramilli, A.S., D'Oliveira, A., Alford, T.L., Boffito, D.C. and Patience, G.S. (2020) Experimental Methods in Chemical Engineering: X-Ray Diffraction Spectroscopy—XRD. *The Canadian Journal of Chemical Engineering*, **98**, 1255-1266. https://doi.org/10.1002/cjce.23747

[25] Fatimah, S., Ragadhita, R., Husaeni, D.F.A. and Nandiyanto, A.B.D. (2021) How to Calculate Crystallite Size from X-Ray Diffraction (XRD) Using Scherrer Method. *ASEAN Journal of Science and Engineering*, **2**, 65-76. https://doi.org/10.17509/ajse.v2i1.37647

[26] ASTM (2018) Standard Test Method for Compressive Strength of Cylindrical Concrete Specimens.

[27] ASTM (2023) Standard Practice for Use of Unbonded Caps in Determination of Compressive Strength of Hardened Concrete Cylinders.

[28] Paredes, D. and Jiménez, E. (2022) Uso de alófano en hormigón para mejorar su resistencia y tiempo de vida.

[29] ASTM (2017) Standard Test Method for Unconfined Compressive Strength of Intact Rock Core Specimens.

[30] ASTM (2020) Standard Test Method for Measurement of Rate of Absorption of Water by Hydraulic-Cement Concretes.

[31] Andreo, S., Tutor, J., Cuquerella, M., Cotutor, J. and Garcia, R. (2022) Universitat Politècnica De València Instituto Universitario Mixto de Tecnología Química Síntesis de materiales microporosos para adsorción de gases.

[32] Mohajerani, A., Burnett, L., Smith, J.V., Kurmus, H., Milas, J., Arulrajah, A., *et al.* (2019) Nanoparticles in Construction Materials and Other Applications, and Im-

plications of Nanoparticle Use. *Materials*, **12**, Article 3052. https://doi.org/10.3390/ma12193052

[33] Wang, Y., Li, L., An, M., Sun, Y., Yu, Z. and Huang, H. (2022) Factors Influencing the Capillary Water Absorption Characteristics of Concrete and Their Relationship to Pore Structure. *Applied Sciences*, **12**, Article 2211. https://doi.org/10.3390/app12042211

[34] Rodríguez Diez, J. (2019) Contratos Especiales. *Revista chilena de derecho privado*, **32**, 147-155. https://doi.org/10.4067/s0718-80722019000100147

[35] Ajay, V. and Rajeev, C. (2012) Effect of Micro Silica on the Strength of Concrete with Ordinary Portland Cement. *Research Journal of Engineering Sciences*, **1**, 1-4.

[36] Li, Z., Cornelis, J., Linden, C.V., Van Ranst, E. and Delvaux, B. (2020) Neoformed Aluminosilicate and Phytogenic Silica Are Competitive Sinks in the Silicon Soil-Plant Cycle. *Geoderma*, **368**, Article 114308. https://doi.org/10.1016/j.geoderma.2020.114308

[37] Silva-Yumi, J., Cazorla Martínez, R., Serrano, C.M. and Lescano, G.C. (2021) Alofán, Una Nanopartícula Natural Presente En Andisoles Del Ecuador, Propiedades Y Aplicaciones Allophane, A Natural Nanoparticle Present in Andisoles of Ecuador, Properties and Applications. https://doi.org/10.17163/lgr.n33.2021.05

[38] Slovenian Institute for Standardization (2023) SIST-EN-ISO-80004-1-2023.

[39] Hakim, L., Dirgantara, M. and Nawir, M. (2019) Karakterisasi Struktur Material Pasir Bongkahan Galian Golongan C Dengan Menggunakan X-Ray Difraction (X-RD) Di Kota Palangkaraya. *Jurnal Jejaring Matematika dan Sains*, **1**, 44-51. https://doi.org/10.36873/jjms.v1i1.136

[40] Nandiyanto, A.B.D., Oktiani, R., Ragadhita, R., Sukmafitri, A. and Zaen, R. (2020) Amorphous Content on the Photocatalytic Performance of Micrometer-Sized Tungsten Trioxide Particles. *Arabian Journal of Chemistry*, **13**, 2912-2924. https://doi.org/10.1016/j.arabjc.2018.07.021

[41] Airlangga, T.A., Matsue, N., Hanudin, E. and Johan, E. (2020) Phosphate Adsorption Capacity of Allophane from Two Volcanic Mountains in Indonesia. *Journal of Tropical Soils*, **25**, 39-46. https://doi.org/10.5400/jts.2020.v25i1.39-46

[42] Du, P., Yuan, P., Liu, J., Yang, Y., Bu, H., Wang, S., *et al.* (2020) Effects of Environmental Fe Concentrations on Formation and Evolution of Allophane in Al-Si-Fe Systems: Implications for Both Earth and Mars. *Journal of Geophysical Research: Planets*, **125**, e2020JE006590. https://doi.org/10.1029/2020je006590

[43] Wang, S., Du, P., Yuan, P., Liu, Y., Song, H., Zhou, J., *et al.* (2020) Structural Alterations of Synthetic Allophane under Acidic Conditions: Implications for Understanding the Acidification of Allophanic Andosols. *Geoderma*, **376**, Article 114561. https://doi.org/10.1016/j.geoderma.2020.114561

[44] la Manna, L.A., Buduba, C.G. and Irisarri, J.A. (2020) Volcanic Soils of Chubut Province, Patagonia, Argentina.

[45] Sanz, D. (2022) El Reto Del Material=The Challenge of the Materia.